Understanding and Mitigating Reactivity of LSM with YSZ

Kyle M. McDevitt[1], Boxun Hu[2], Manoj K. Mahapatra[2], Vinit Sharma[2], Rampi Ramprasad[2], Nguyen Minh[3], Prabhakar Singh[2], and Scott T. Misture[1]
[1]The Inamori School of Engineering, Alfred University, Alfred, NY 14802 [2]University of Connecticut [3]University of California San Diego

Overview: *Mitigating Mn destabilization of YSZ*

- Reaction mechanisms in the YSZ-LSM system are dependent on atmosphere.[1] Powder mixture compacts were annealed in air, humid air, and 10% CO_2 in air to study reaction mechanisms and phase evolutions

Four LSM chemistries:

$La_{0.8}Sr_{0.2}MnO_{3-\delta}$	**(LSM-20)**	**Praxair**
$La_{0.8}Sr_{0.1}Ca_{0.1}MnO_{3-\delta}$	**(LSM+Ca)**	Synthesized
$La_{0.8}Sr_{0.2}Mn_{0.7}Ni_{0.3}O_{3-\delta}$	**(LSM+Ni)**	Synthesized
$La_{0.8}Sr_{0.1}Ca_{0.1}Mn_{0.7}Ni_{0.3}O_{3-\delta}$	**(LSM+Ca+Ni)**	Synthesized

LSM bulk phase transition

- Annealing at high temperatures facilitates formation of the orthorhombic (Pnma) LSM phase for Ca-containing forms.

  → Attributed to smaller A-site cation increasing octahedral tilting, to enhance the effects of the Mn^{3+} Jahn-Teller distortion[2]

- Transformation was observed immediately in Ca containing samples, and gradually in the Ca+Ni containing samples. Latter remains unclear, perhaps Ni^{3+} redistribution (large J-T distortion in LS state).

A-site ion	Radius (Å)
La^{3+}	1.36
Ca^{2+}	1.34
Sr^{2+}	1.44

B-site ion	Radius (Å)
Mn^{3+} (Low spin)	0.58
Mn^{3+} (High spin)	0.645
Mn^{4+}	0.53
Ni^{2+}	0.69
Ni^{3+} (Low spin)	0.56
Ni^{3+} (High spin)	0.60
Ni^{4+}	0.48

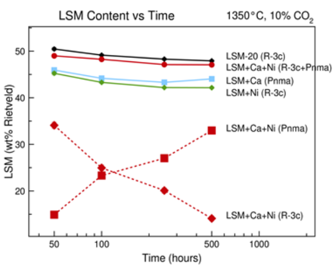

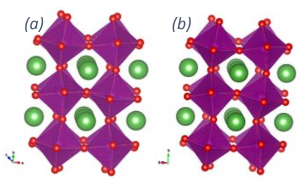

Rhombohedral LSM (a) vs orthorhombic LSM (b). In a, the Mn-O-Mn bond angle is 163.8°, while in b, the angle is 162.2°.

- XPS peak shape[3] suggests that the chemistries tending to form the Pnma phase have a lower ratio of Mn^{4+} to Mn^{3+}.
  → Agrees with the *x* vs. pO_2 phase diagram generated by Mitchell et al[2] as well as observations from Rørmark et al.[4]

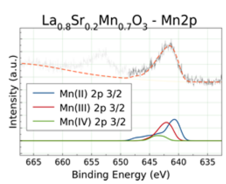

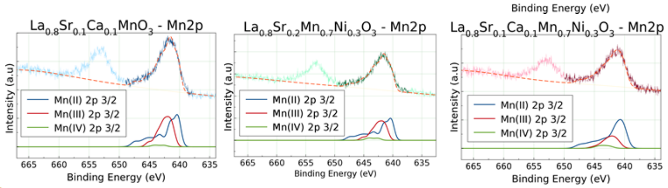

Water Inhibits Degradation via Lanthanum Zirconate

- $La_2Zr_2O_7$ formation occurs in both air and CO_2 rich air.[5,6]
- Ni containing samples formed the most $La_2Zr_2O_2$ in both atmospheres.
- $La_2Zr_2O_7$ did not form after annealing for 500 hours in humid air.

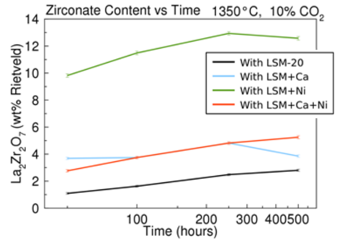

Intentional Mn diffusion profile

- Mn shows appreciable solubility in YSZ.[5]
- XRD on both sides of the pellet indicate qualitatively that more $La_2Zr_2O_7$ forms on the Mn deficient side.

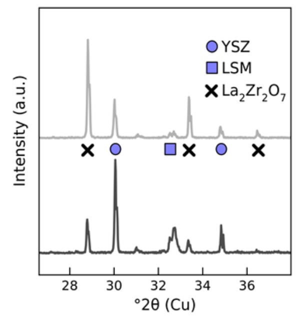

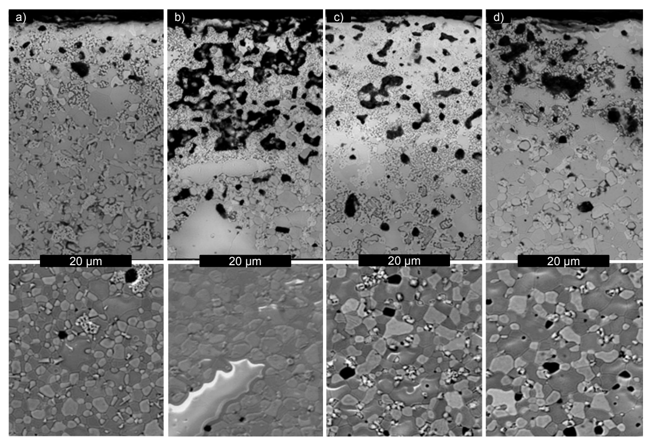

a) YSZ-LSM-20 **b) YSZ–LSM+Ca** **c) YSZ–LSM+Ni** **d) YSZ–LSM+Ca+Ni**
(500h at 1350°C in 10% CO_2)

- Significant reaction was observed at the interface exposed to YSZ powder.
- $La_2Zr_2O_7$ forms as fine-grained crystals with high contrast.

Zirconia Phase Destabilization

- Mn destabilizes the cubic phase and destroys conductivity, ultimately compromising functionality of the SOFC.[1,5,7]
- Increasing stability of the LSM may improve long-term LSM-YSZ stability. → Possible with Ca and Ni additions.

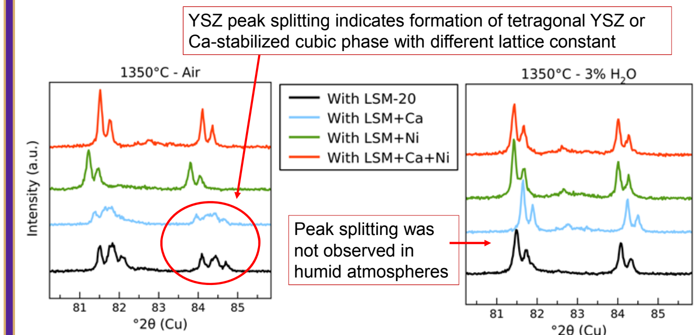

	LSM-20	LSM + Ca	LSM +Ni	LSM +Ca+Ni
Air	**Unstable** (Tetragonal YSZ)	**Unstable** (Forms CSZ)	**Stable**, but with $La_2Zr_2O_7$	**Stable**
10% CO_2 90% Air	**Unstable** (Tetragonal YSZ)	**Unstable** (Forms CSZ)	**Stable**, but with $La_2Zr_2O_7$	**Stable**
Humid air (3% H_2O)	**Stable**	**Stable**	**Stable**	**Stable**

Conclusions

- Combined Ca and Ni additions yield highest-stability LSM
  - In part thermodynamic
  - Potential for B-site deficient LSM to be more stable against YSZ
  - Goal is to stabilize the Mn ion in the LSM – Ni addition is effective
- Mn diffusion from LSM is responsible for both zirconia destabilization and formation of $La_2Zr_2O_7$.[1] This reaction is inhibited by water.
  - **Anion** substitutions that force Mn to charge compensate: OH^- from humid air on O^{2-} site

LSM+Ca+Ni Recommended for Long-Term Testing

References

1. M. Chen, Y.-L. Liu, A. Hagen, P. V. Hendriksen, and F.W. Poulsen, "LSM-YSZ Reactions in Different Atmospheres," Fuel Cells, 9 [6] 833–840 (2009).
2. J.F. Mitchell, D.N. Argyriou, C.D. Potter, D.G. Hinks, J.D. Jorgensen, and S.D. Bader, "Structural phase diagram of $La_{1-x}Sr_xMnO_3$: Relationship to magnetic and transport properties," Phys. Rev. B, 54 [9] 6172–6183 (1996).
3. M. Biesinger, B. Payne, and A. Grosvenor, "Resolving surface chemical states in XPS analysis of first row transition metals, oxides and hydroxides: Cr, Mn, Fe, Co and Ni," Appl. Surf. Sci., 257 [7] 2717–2730 (2011).
4. L. Rørmark, K. Wiik, S. Stølen, and T. Grande, "Oxygen stoichiometry and structural properties of $La_{1-x}A_xMnO_{3\pm\delta}$ (A = Ca or Sr and $0 \le x \le 1$)," J. Mater. Chem., 12 [4] 1058–1067 (2002).
5. H. Yokokawa, N. Sakai, T. Kawada, and M. Dokiya, "Thermodynamic Analysis on Interface Between Perovskite Electrode and YSZ Electrolyte," Solid State Ionics, 398–401 (1990).
6. C. Levy, Y. Zhong, C. Morel, and S. Marlin, "Thermodynamic Stabilities of $La_2Zr_2O_7$ and $SrZrO_3$ in SOFC and Their Relationship with LSM Synthesis Processes," J. Electrochem. Soc., 157 [11] B1597-B1601 (2010).
7. V.A. Cherepanov, L.Y. Barkhatova, and V.I. Voronin, "Phase Equilibria in the La–Sr–Mn–O System," J. Solid State Chem., 134 [1] 38–44 (1997).

Alfred University
The Inamori School of Engineering

This work was supported by DOE under grant number DE-FE-9682.
The valuable comments and guidance of Briggs White are also acknowledged.